

Structural, Thermal and Electrical Properties of Nano Manganese-Composite Polymer Electrolytes

Mohd Rafie Johan, Lim May Ting

Advanced Materials Research Laboratory, Department of Mechanical Engineering, University of Malaya, Lembah Pantai, 50603 Kuala Lumpur, Malaysia

*E-mail: mrafiej@um.edu.my

Received: 25 June 2011 / Accepted: 6 September 2011 / Published: 1 October 2011

We synthesized a new kind of solid polymer electrolyte with polyethylene oxide (PEO) as a host, lithium triflate (LiCF_3SO_3) as a salt, dibutyl phthalate (DBP) as a plasticizer and nanomanganese (MnO_2) as a filler using solution cast technique. Nanomanganese was produced through mechanical milling process with a size in range of 60-80 nm as shown by TEM image. XRD patterns confirmed the complex formation of PEO- LiCF_3SO_3 -DBP- MnO_2 system. The optimum conductivity value at room temperature was $4.2 \times 10^{-4} \text{ Scm}^{-1}$ for 12 wt% of MnO_2 . The ionic conductivity of the polymer electrolytes show increases with temperature and obey the Arrhenius law. The XRD and DSC studies indicate that the conductivity increase is due to the increase of the amorphous content which enhances the segmental flexibility of polymeric chains and the disordered structure of the electrolyte.

Keywords: Nanocomposites polymer electrolyte; Solution casting; Inorganic filler; Ionic conductivity; Milling

1. INTRODUCTION

There has been increasing interest in the development of solid polymer electrolytes (SPE) due to their potential applications in solid-state electrochemical devices and in particular in solid-state rechargeable lithium batteries [1-2]. SPE have many advantages, namely high ionic conductivity, high specific energy, a solvent free condition, wide electrochemical stability windows, light and easy processability [3-6]. In most SPE, the polymer host is doped with inorganic salts in order to enhance the conductivity. The ionic conductivity is due to mobility of the conducting species contributed by the inorganic salt which dissociated into ions. The ions in the film migrated primarily through the solvents which in turn contributed to the conductivity enhancement [7]. However, the ionic conductivity of PEO-salts at ambient temperature is rather low due to the crystallinity of the PEO [8-9]. NMR studies

indicate that the ion transport occurs in the amorphous regions of the polymer and taken together with temperature dependence measurements implicate polymer segmental motion in the conduction mechanism [10]. High ionic conductivities can only be obtained beyond the melting point of PEO. Thus considerable effort has been directed at enhancing the ionic conductivity of the polymer electrolytes. A common approach is to add plasticizers to a polymer matrix. This leads to a high ambient conductivity but promotes deterioration of the electrolyte's mechanical properties. However, the addition of inorganic filler to the polymer matrix improved the mechanical stability and enhanced ionic conductivity [5,11-13].

The fillers affect the PEO dipole orientation by their ability to align dipole moments, while the thermal history determines the flexibility of the polymer chains for ion migration [14-15]. The addition of fillers generally improves the transport properties, the resistance to crystallization and the stability of the electrode/electrolyte interface [12,15-16]. Meanwhile, the type of filler and its particle size will influence the conductivity [17-20].

Therefore, the study of the combined effect of the salt, plasticizer and filler onto PEO would be of great interest. In light of all this, present work has been driven in achieving high ionic conductivity and mechanical stabilities of nanocomposite polymer electrolyte.

2. EXPERIMENTAL

Polymer electrolyte films were prepared using solution-cast technique. Poly-ethylene oxide (PEO with 600,000 mw Acros Organics) was used as host polymer matrix, lithium triflate (LiCF_3SO_3 -Alfa Aesar) as the doping salt, dibutyl phthalate (DBP- Alfa Aesar) as plasticizer and manganese (MnO_2) as filler. LiCF_3SO_3 was dried at 100°C for an hour prior to use due to its hygroscopic characteristic [20]. Subsequently, PEO and LiCF_3SO_3 were dissolved separately in acetonitrile and then mixed together and stirred in a closed container.

The results were then poured into the glass petri dishes and allowed to dry at room temperature. The films were then stored in the desiccator. In order to investigate the effect of plasticizers on the PEO - salt samples, the highest conducting PEO-salt sample was added with dibutyl phthalate (DBP). The previous similar procedures were carried out added with various wt% of DBP. To investigate the effect of nano-ceramic fillers to the PEO-salt-plasticizer samples, MnO_2 was added to the highest conducting PEO - salt-plasticizer sample.

Nano-ceramic filler was prepared by mechanical milling process for 48 hrs using the planetary ball mill. The particle size and distribution were examined using Transmission Electron Microscope (TEM LIBRA 120) operating at 120 kV. The X-ray diffraction (XRD) patterns of the films were obtained using Phillips X-pert MRD X-ray diffractometer. The Differential Scanning Calorimetry (DSC) of the films were carried out using Mettler DSC 820 Calorimeter at a heating rate of $10^\circ\text{C min}^{-1}$ and -100 to 0°C . Conductivity measurements were carried out using the Impedance Spectroscopy HIOKI 3531 LCR in the frequency range from 50 Hz – 1 MHz with temperature ranging from room temperature up to 100°C .

3. RESULTS AND DISCUSSION

3.1. Analysis of ceramic filler

Fig. 1 shows the TEM image of milled MnO_2 . It is clearly showed of assemblies of nanosized particles. However, the diameter of these particles is not uniform throughout. The most probable sizes were found in the range of 12 to 15 nm as shown in Fig. 2.

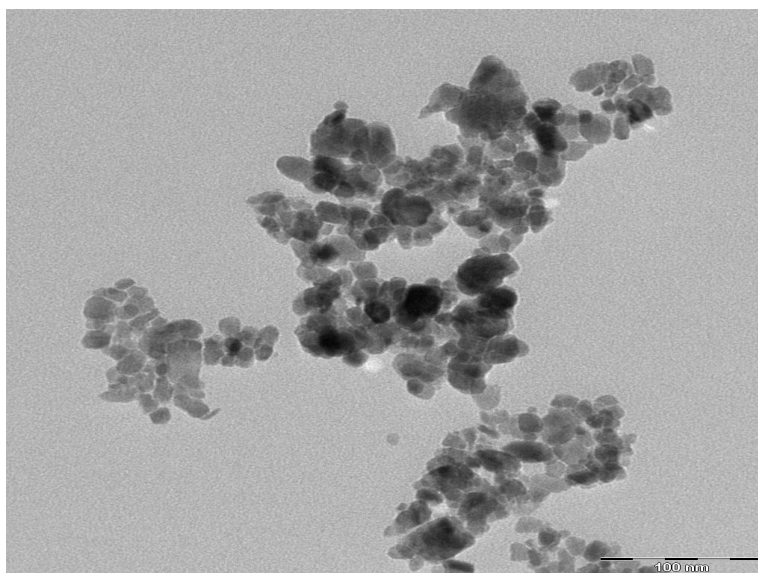


Figure 1. TEM image of MnO_2

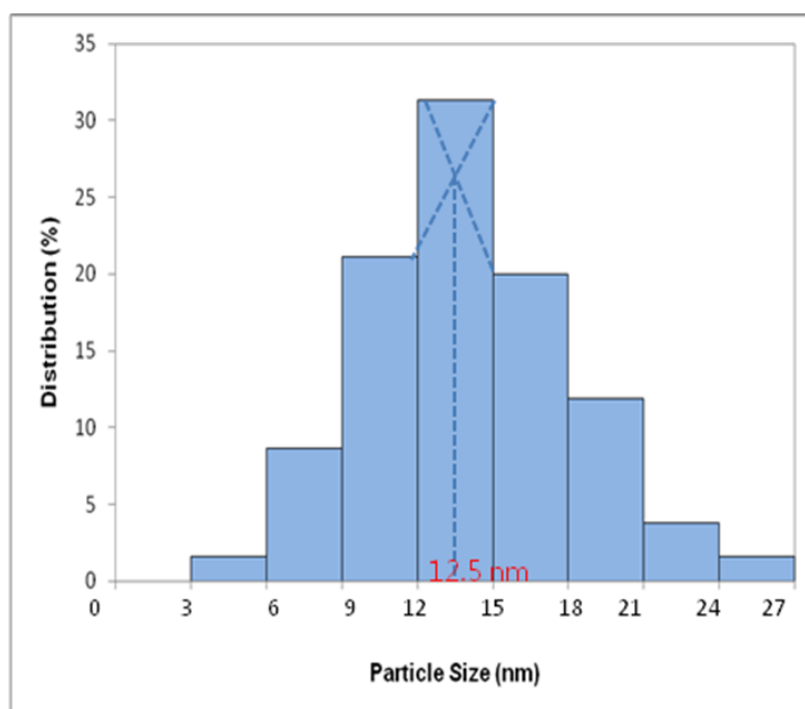


Figure 2. Particle size distribution of nano-manganese

3.2. XRD Analysis

Fig. 3 shows the XRD patterns for MnO₂ particles after milling. The crystallite size of MnO₂ particle was calculated using Scherer equation below:

$$L = \frac{0.9\lambda}{\beta \cos \theta} \quad (1)$$

where L is the crystallite size, λ is the X-ray wavelength, θ is the diffraction angle and β is the full width at half-maximum (FWHM). The crystallite size value is 11.7 nm and in a good agreement with the TEM result.

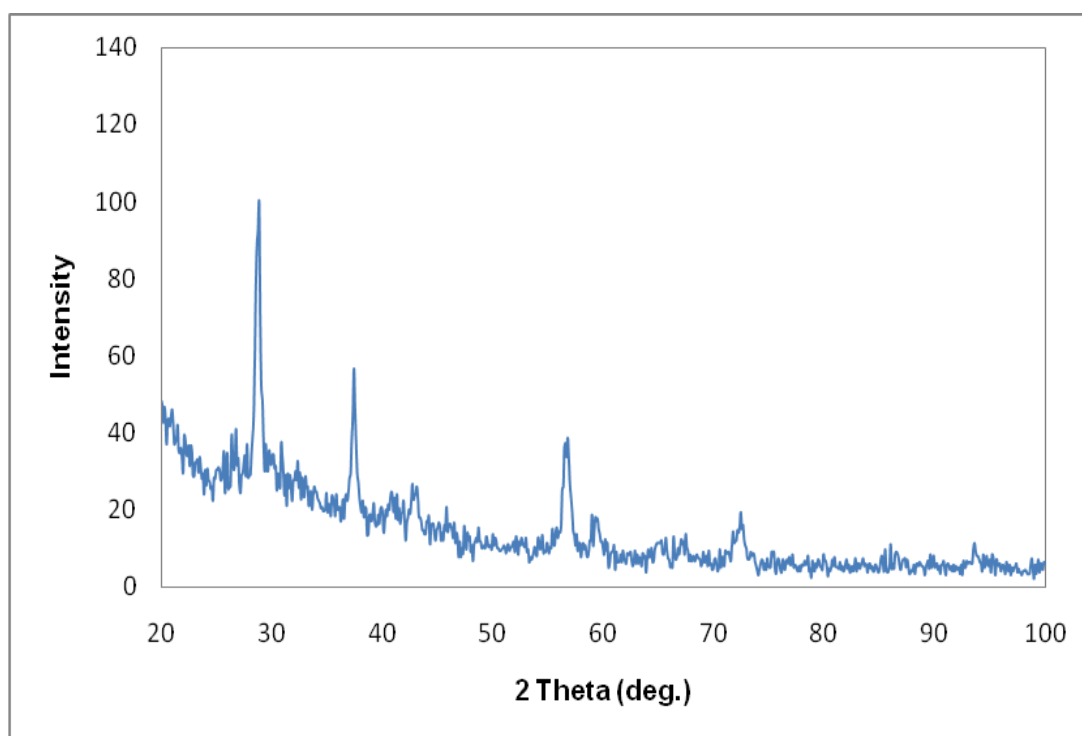


Figure 3. XRD pattern for MnO₂ nanoparticle

Fig. 5 displays the XRD patterns for polymer electrolyte complexes. The sample is partially crystalline with a sharp PEO peak at $2\theta = 19.41^\circ$ and 23.51° . However, the sample shows a decrease in the PEO peaks after the addition of salt to PEO. This indicates the decrease of the degree of crystallinity which originates from the ordering of polyether side chains. In a typical EO chain containing lithium ion conducting electrolyte, there is an optimum salt concentration at which a maximum conductivity appears. At lower salt concentration, the build-up of charge carriers with the increase of salt concentration leads to an increase in ionic conductivity. However, this will be offset by the formation of ion clusters and decrease of chain flexibility at higher salt concentration. When LiCF₃SO₃ salt is incorporated into polymer PEO matrices, changes of the diffraction peaks of salts is

observed which indicates that the salt has been solvated. Moreover, when plasticizer, EC was added, there is reduction observed in intensity of the peaks relative to pure PEO. This indicates that the polymer complexation has taken place between PEO and LiCF_3SO_3 , and DBP, which also promotes amorphous region to the polymer structure. The trend is continues when adding MnO_2 into the plasticized PEO- LiCF_3SO_3 complex. It is evident that the crystalline peaks have decreased sharply upon addition of MnO_2 and composition consists predominantly of an amorphous nature.

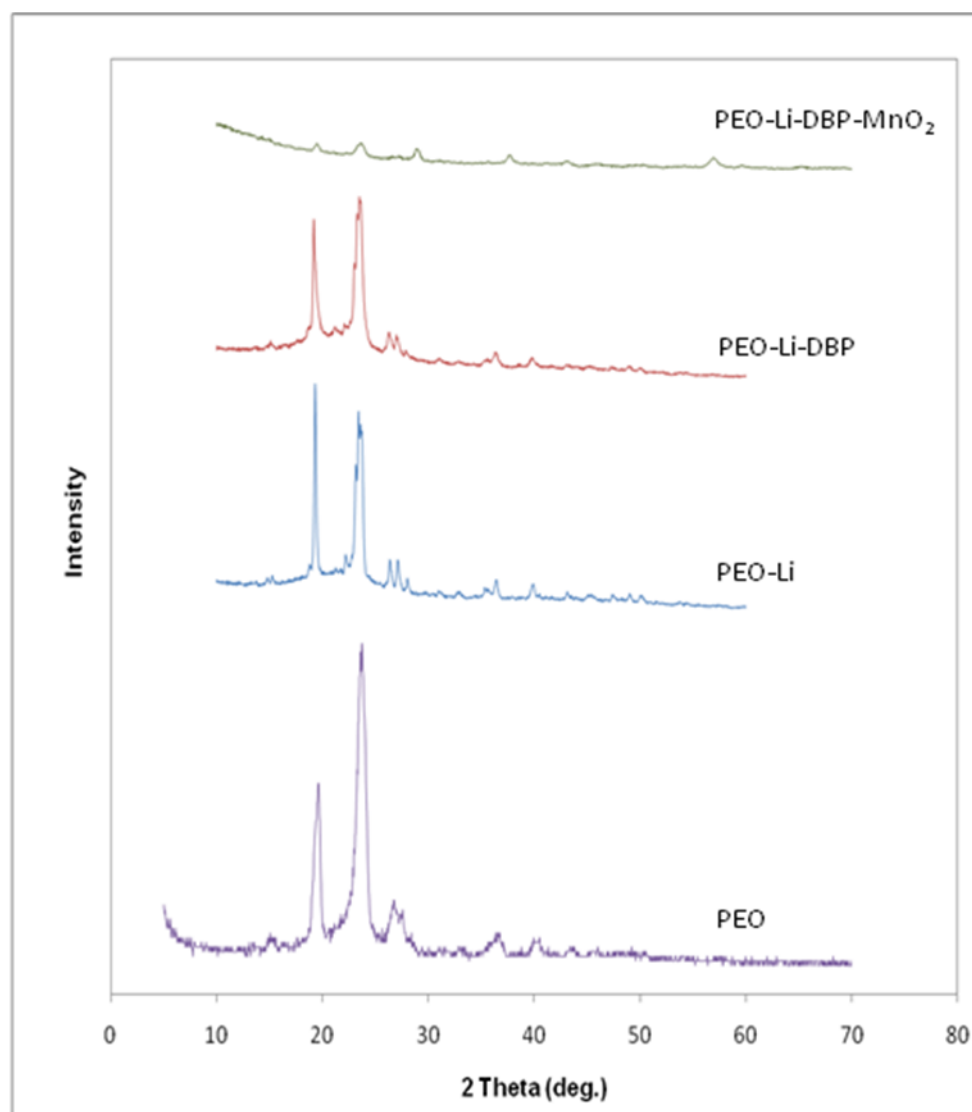


Figure 4. XRD patterns of (a) pure PEO; (b) PEO- LiCF_3SO_3 ; (c) PEO- LiCF_3SO_3 -DBP; (d) PEO- LiCF_3SO_3 -DBP- MnO_2 complexes

3.3. Thermal Studies

Fig. 5 shows the DSC thermograms of the different polymer electrolyte samples incorporating lithium triflate salt, plasticizer (DBP) and manganese filler. These results clearly show that both the glass transition temperature (T_g) and the melting temperature (T_m) have decreased due to the addition

of the salt and plasticizer. Table 1 summarizes the the DSC results of the nano-composite polymer electrolyte samples. These observations clearly suggest that a major contribution to the conductivity enhancement comes from the structural modifications associated with the polymer host caused by the plasticizers. However, T_g was increased slightly to -70°C with the addition of MnO_2 but the temperature is still below the pure PEO glass transition temperature. So the ionic conductivity would still increase due to the addition of manganese. In the meantime, the increase of T_g in this sample shows that the polymer electrolyte is stable which difficult to change phase from amorphous to crystal state when heated and this would correlate to the improvement in mechanical properties.

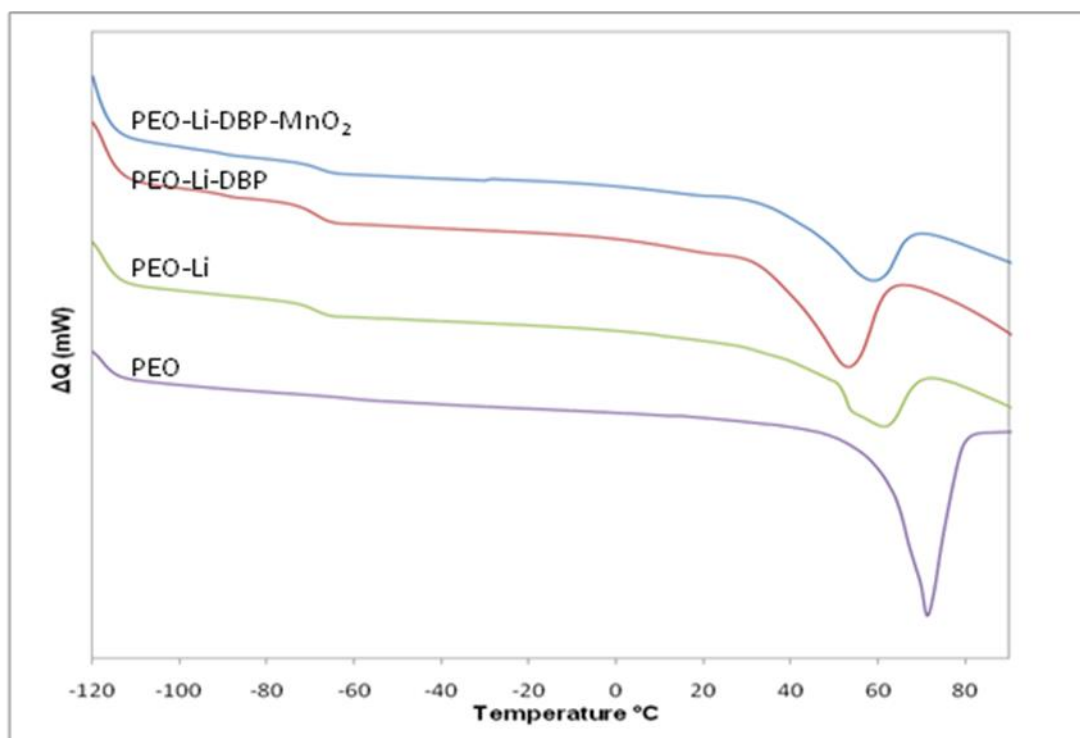


Figure 5. DSC thermograms of (a) pure PEO; (b) PEO- LiCF_3SO_3 ; (c) PEO- LiCF_3SO_3 -DBP; (d) PEO- LiCF_3SO_3 -DBP- Al_2O_3 complexes

Table 1. Glass transition temperature, melting point and crystallinity of each polymer electrolyte complex

Polymer Electrolyte	T_m ($^\circ\text{C}$)	T_g ($^\circ\text{C}$)	χ_c (%)	Activation energy (eV)	
				298 - 328 (K)	328 - 373 (K)
PEO	70	-65	78.5	0.53	0.29
PEO- LiCF_3SO_3	61	-71	38.1	0.27	0.13
PEO- LiCF_3SO_3 -DBP	43	-74	42.9	0.18	0.10
PEO- LiCF_3SO_3 -DBP- MnO_2	58	-70	21.7	0.17	0.05

The increase of the amorphous phase content can be clearly seen (Table 1) by calculating the relative percentage of crystallinity (χ_c) for the electrolyte samples studied. The relative percentage of crystalline PEO, χ_c , can be calculated using the equation below:

$$\chi_c = \frac{\Delta H_m^{complex}}{\Delta H_m^*} \times 100\% \tag{2}$$

where ΔH_m^* is the heat of fusion of PEO. It can be clearly seen that in Table 1, χ_c decreases due to the salt, plasticizer as well as the filler. This is a good evidence to estimate the enhancement of volume fraction of the amorphous phase caused by the modification of the polymer–salt matrix after the addition of the plasticizer and filler.

3.4 Ionic Conductivity

The conductivity of the PEO-LiCF₃SO₃, PEO-LiCF₃SO₃-EC, PEO-LiCF₃SO₃—DBP and PEO-LiCF₃SO₃-DBP-MnO₂ systems at room temperature is illustrated in Figs. 6-8. Fig. 6 shows that conductivity increases with increase in LiCF₃SO₃ content. The highest conductivity is observed for the sample containing 15wt% LiCF₃SO₃ at $3.3 \times 10^{-6} \text{ Scm}^{-1}$. As the salt content increases, the number density of mobile ions η in the electrolyte increases. From the Rice and Roth model [22] that express the ionic conductivity σ as

$$\sigma = \frac{2}{3} \left[\frac{(Ze)^2}{k_B T m} \right] \eta E_A \tau \exp\left(-\frac{E_A}{k_B T}\right) \tag{3}$$

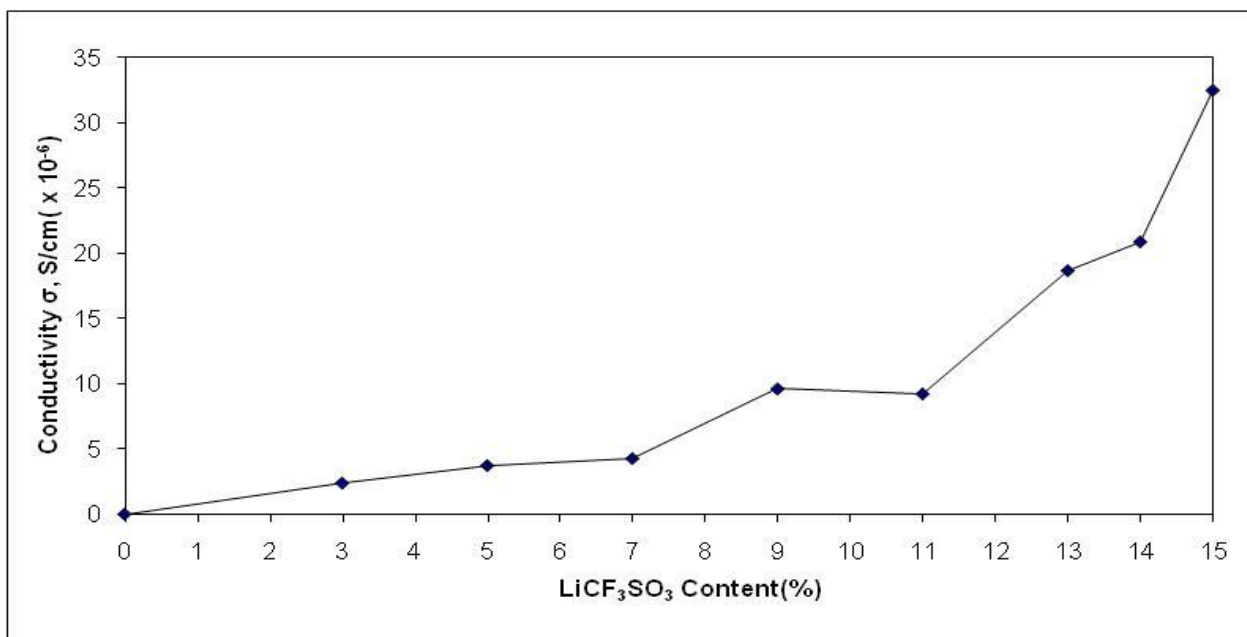


Figure 6. Conductivity of PEO as a function of LiCF₃SO₃ content at room temperature

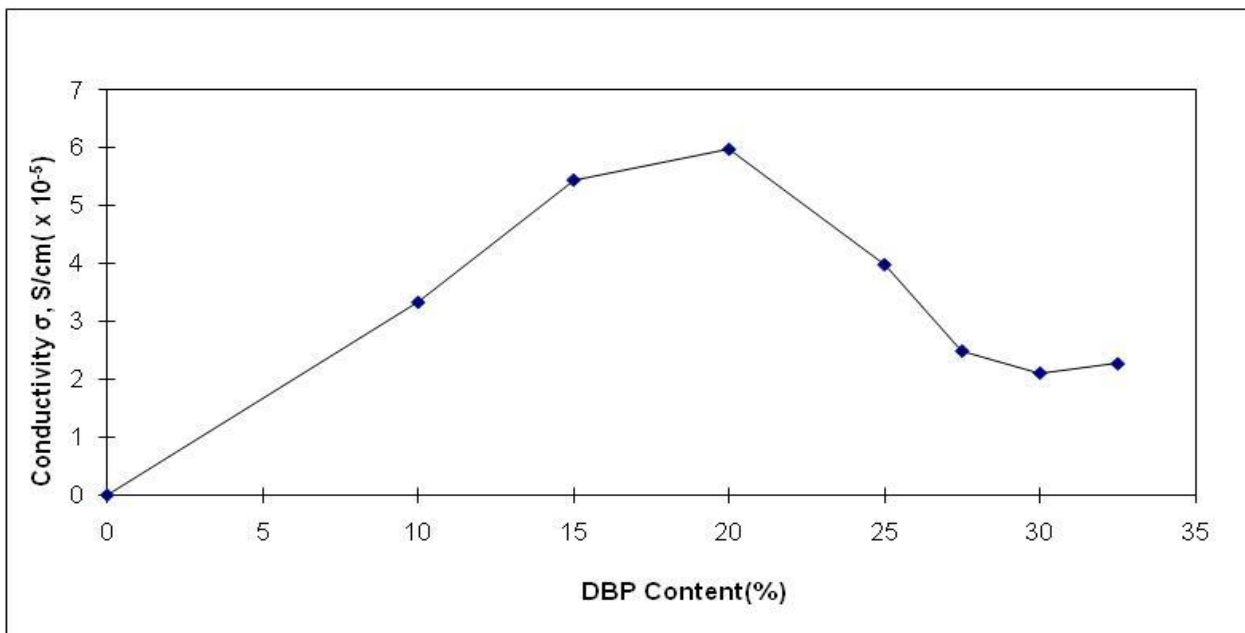


Figure 7. Conductivity of PEO-LiCF₃SO₃ as a function of DBP content at room temperature

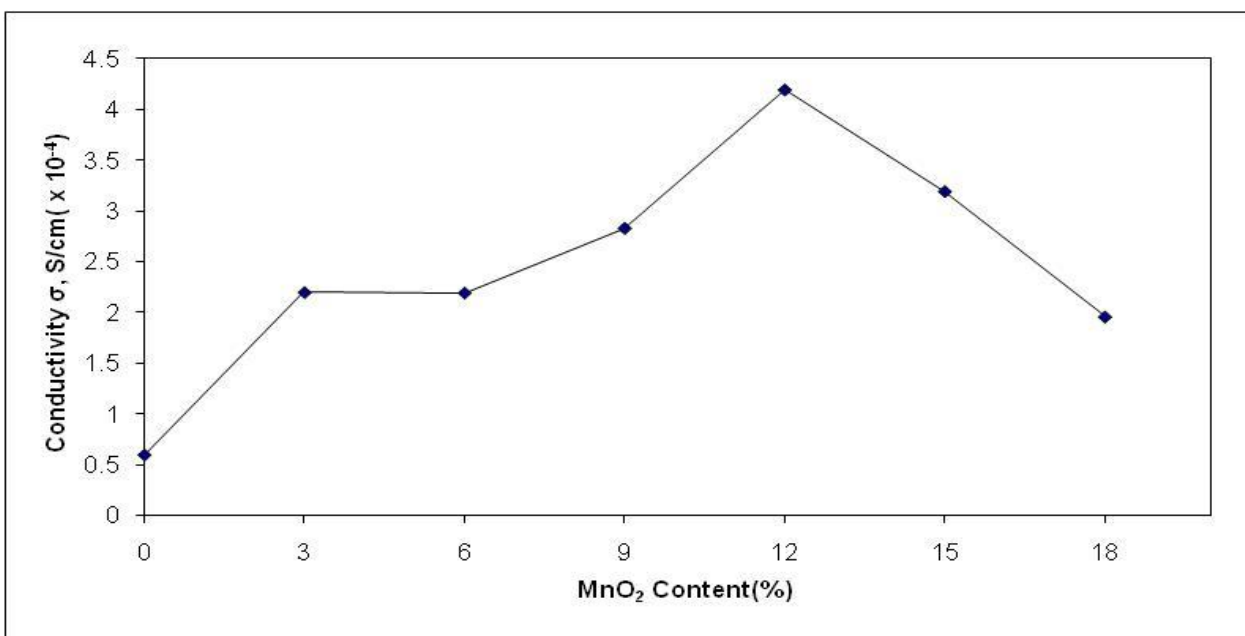


Figure 8. Conductivity of PEO-LiCF₃SO₃-DBP as function of MnO₂ content at room temperature

Where Z , E_A and m is the valency, activation energy and mass of the conducting ion, respectively. T is absolute temperature, k_B is Boltzman constant and e is the electronic charge and τ is a time to travel between sites. The conductivity is expected to increase when η increases. However, at higher composition of LiCF₃SO₃ (beyond 15%), it fails to form thin film and remained in gel-like state. This may be caused by the presence of water molecules since LiCF₃SO₃ salt has a very strong ability

to absorb water molecules. As a result, water molecules form hydrogen bonding with PEO and interrupt the linkage forming between PEO–LiCF₃SO₃ systems.

Fig. 7 shows the effect of DBP on the conductivity of the highest conducting PEO-LiCF₃SO₃ sample. DBP does not supply ions to the electrolyte system but is able to dissociate more salts into ions and has a low viscosity that can increase ionic mobility. The dissociation condition of the salt and the carrier mobility are dominated by the polymer and solution. With increasing plasticizer content, the dielectric constant for the film increases and increased its ability to dissolve the salt [19, 23–25]. It can be observed that conductivity of sample increases to $6.0 \times 10^{-5} \text{ Scm}^{-1}$ at 20 wt% DBP. This is because most of the DBP molecules are involved in shielding the hydrogen and oxygen atoms from interacting, while the remaining DBP molecules (which are not many in number) are involved in reducing the coulombic interaction between the anions and cations of the salt [26]. This leads to increase in conductivity. The addition of more than 20 wt% DBP decreases the ionic conductivity of the polymer. This is attributed to the formation of linkages between the plasticizer itself and causing it to crystallize resulting in the decrease in ionic conductivity [27–29]. Fig. 8 shows the effect of MnO₂ nanofiller on the conductivity of the highest conducting PEO-LiCF₃SO₃-DBP sample. It is observed that the conductivity in SPE does not vary linearly with the amount of the filler. According to Lewis acid-base model [17], the addition of MnO₂ as filler increases the ionic conductivity of SPE synergistically by inhibiting the recrystallization of PEO chains and providing Li⁺ conducting pathways at the filler surface through Lewis acid-base interaction among different species in the SPE. The ion movement is obstructed by the crystalline region present in SPE while blocking the paths of the ions.

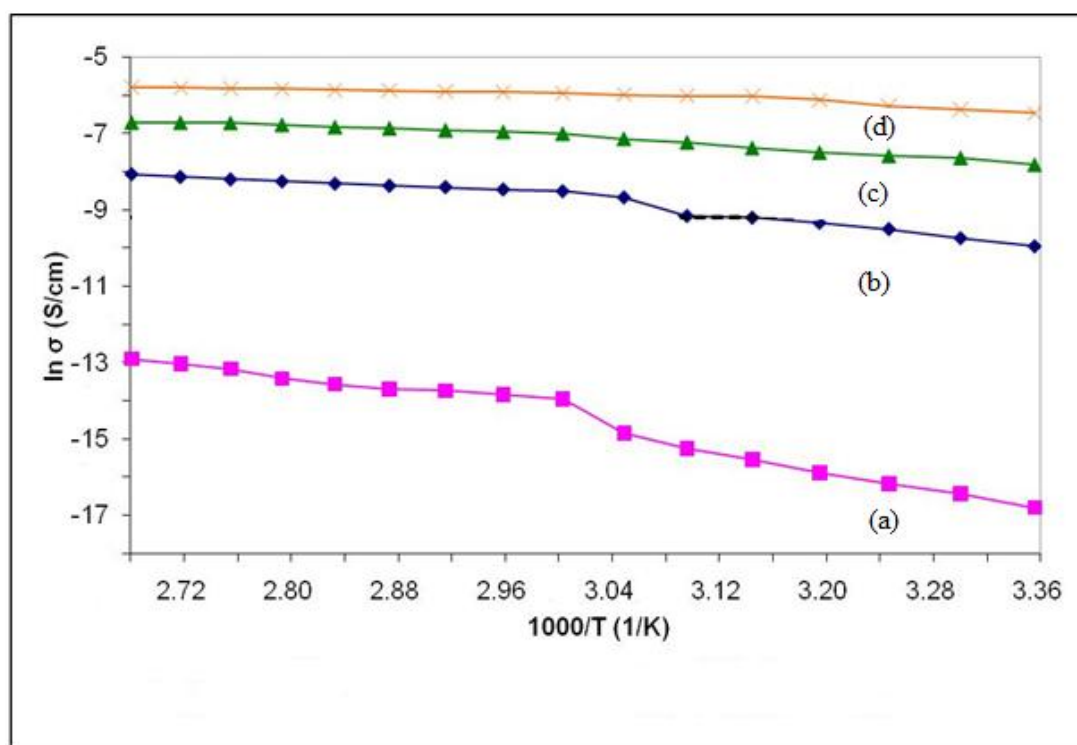


Figure 9. Temperature dependence conductivity of (a) pure PEO; (b) PEO-LiCF₃SO₃; (c) PEO-LiCF₃SO₃-DBP; (d) PEO-LiCF₃SO₃-DBP-Al₂O₃ complexes

The amorphous region on the other hand favours the conduction of Li^+ ion due to its greater free volume. The larger surface area of this finely divided MnO_2 filler prevents the local PEO chain reorganization, leading to locking in high degree of disorder and enhancing thereby the ionic conductivity of SPE. The presence of nano MnO_2 filler has enhanced the ionic conductivity to $\sigma = 4.2 \times 10^{-4} \text{ Scm}^{-1}$ at 12 wt% of MnO_2 .

The Arrhenius plot for each complex is shown in Fig.9. A closer inspection of this figure reveal that the conductivities of both the amorphous phase above T_m and the partly crystalline phase below T_m have increased substantially due to the presence of the salt, plasticizer and ceramic filler. The discontinuity in the figure is due to the phase change of PEO from crystalline to the amorphous phase (T_m). It is well established that the ion conduction in the amorphous phase of the polymer complex is higher compared to the crystalline phase. The sudden enhancement in the conductivity T_m is, thus, interpreted as due to the crystalline melting of the PEO. The presence of the crystalline phase very much hampers the segmental motion of the PEO chains in the amorphous phase. Thus, a melting of the crystalline phase improves the dynamic properties of the polymer electrolytes resulting in an enhancement in the ion conduction. In the case of pure PEO and PEO- LiCF_3SO_3 complexes, the polymer chains are rigid and less mobile and, hence, the phase transformation temperature region (T_m) is seen distinctly. However, the two distinct and well-separated regions (below and above T_m) gradually merges when the plasticizer and filler is added to the system. This may be due to the fact that the plasticizer and filler preferentially interact with the crystalline PEO, thereby reducing the content of the crystalline phase in the polymer electrolyte. However, the discontinuity in the plots around T_m becomes less visible for the addition of plasticizer and filler that correspond to higher conductivities. The ionic conductivity increased with increasing temperature as a result of the free volume model where, as the temperature increases, the polymer electrolyte can expand easily and produces free volume. Therefore, ions, solvated molecules, or the polymer segments can move into the free volume, causing it to increase. This enhances the ion and polymer segmental mobility that will, in turn, enhance the ionic conductivity. The conductivity in the filler-added system is higher than that in the plasticized system and always showed the highest conductivity from 298 to 373 K. This conductivity enhancement at temperatures above as well as below T_m , should therefore be caused by a different mechanism directly associated with the surface groups in the filler grains. This conductivity enhancement possibly results from Lewis acid-base-type oxygen and OH surface groups on manganese grains interact with the cations and anions and provide additional sites creating favorable high conducting pathways in the vicinity of grains for the migration of ions. This is reflected as an increased mobility for the migrating ions. However, an additional substantial contribution to the conductivity enhancement below T_m appears to come from the increased fraction of the amorphous phase retained due to the presence of the filler at these temperatures.

Since the conductivity–temperature data obeys Arrhenius relationship, the nature of cation (Li^+) transport quite similar to that occurring in ionic crystals, where ions jumps into neighboring vacant sites and hence increases the ionic conductivity to a higher value. The activation energy values E_a (Table 1) shows that each system has a higher conductivity and lower activation energy at high temperature. It also can be linked to the decrease in viscosity and increased chain flexibility. The activation energy for ions transport decreases with the addition of plasticizer and filler. It illustrates

that the lower the activation energy, the more easily lithium ion migrate. Furthermore, the increase of the amount of interfacial layers facilitates the migration of lithium ions.

4. CONCLUSION

We have successfully prepared a new PEO composite polymer electrolyte using MnO_2 as a filler and DBP as plasticizer by solution casting technique. The complex formation in PEO- LiCF_3SO_3 -DBP- MnO_2 system has been confirmed from the XRD results. The ionic conductivity enhancement observed in the PEO- LiCF_3SO_3 -DBP- MnO_2 system evidently results from the combined effect of salt, plasticizer and the filler. The optimum conductivity value was $4.2 \times 10^{-4} \text{ Scm}^{-1}$ for at 12 wt% of MnO_2 at room temperature (298 K). The ionic conductivity of the polymer electrolytes show temperature dependence where it increases with the increasing temperature and shows the Arrhenius behavior. Besides, the activation energy decreases with increasing ionic conductivity in high temperature and also decreases with the addition of salt, plasticizer and filler. The increase in conductivity was due to the reduction in the crystalline phase with the addition of salt, plasticizer and filler as evident from the XRD analysis where it show that the intensity of the crystalline peaks of the XRD pattern decreases and the area under the peak was broadening. the conductivity enhancement is largely caused by the reduced glass transition temperature and PEO crystallite melting temperature due to the presence of the salt, plasticizer as well as filler. All of this may be related to a possible enhancement in the segmental flexibility of polymeric chains and the disordered structure of the electrolyte where the lithium ion motion taking place in the amorphous phase is facilitated compared to the pure PEO sample.

ACKNOWLEDGMENTS

The financial support received from Sciencefund (13-02-03-3068), Ministry of Science and Innovation Malaysia is gratefully acknowledged.

References

1. F.M. Gray: Polymer Electrolytes, RSC Materials Monographs, The Royal Society of Chemistry, Cambridge, (1997).
2. J.M. Tarascon, M.Armand: *Nature* 414 (2001) 359.
3. J.Y. Kim, S.H. Kim: *Sol. Stat. Ion.* 124 (1/2) (2000) 91.
4. C.H. Manoratne, R.M.G. Rajapakse, M.A.K.L. Dissanayake: *Int. J. Electrochem. Sci.* 1 (2006) 32.
5. H. Zhang, P. Maitra, S.L. Wunder: *Solid State Ionics* 178 (2008) 1975.
6. A.H. Stephan, K.S. Nahm: *Polymer* 47 (2006) 5952.
7. A.K. Arof, S. Ramesh, Tan Winie: *Euro. Poly. Jour* 43 (2007) 1963.
8. Y. Tominaga, N. Takizawa, H. Ohno: *Electrochim. Act.* 45 (2000) 1285.
9. L. Ding, J. Shi, C. Yang, S. Dong: *Poly. Jour.* 29 5 (1997) 410.
10. M.A. Ratner, D. F. Shriver: *Chem. Rev.* 88 (1988) 109.
11. W. Wiczorek, J.R. Stevens, Z. Florjanczyk: *Solid State Ionics* 85 (1996) 67.
12. P.A.R.D. Jayathilaka, M.A.K.L. Dissanayake, I. Albinson, B.E. Mellander: *Electrochim. Act.* 47 (2002) 3257.

13. C.W. Nan, L. Fan, Y. Lin, Q. Cai: *Phy. Rev. Lett.* 91 (2003) 266104.
14. B. Kumar, L. G. Scanlon, R. J. Spry: *J. Power Sources* 96 (2001) 337.
15. K.S. Ji, H.S. Moon, J.W. Kim, J.W. Park: *J. Power Sources* 117 (2003) 124.
16. H.J. Walls, J. Zhou, J.A. Yerian: *J. Power. Sources.* 89 (2000) 156.
17. E. Quartarone, P. Muscarelli, A. Magistris: *Solid State Ionics* 110 (1998) 1.
18. T. Kuila, H. Acharya, S.K. Srivastava, B.K. Samantaray, S. Kureti: *Mater. Sci. Eng.B* 137 (2007) 217.
19. M.R. Johan, B.F. Leo: *Ionics* 16,4 (2010) 335.
20. M. R. Johan, S. A. Jimson, N. Ghazali, N. A. M. Zahari, N.. Redha: *Int. J. Ma. Mat. Res.*102 (2011) 4
21. S. M. Tan, M. R. Johan: *Ionics DOI* 10.1007/s11581-011-0541-7
22. M.J. Rice, W.L. Roth: *J. Sol. Stat. Chem.* 4 (1972) 294.
23. Z. Osman, Z.A. Ibrahim, A.K. Arof, *Carbohydrate Polymers* 44 (2001) 167.
24. M. Kumar, S.S. Sekhon, *Ionics* 8 (2002) 223.
25. S. Ramesh, O.P. Ling, *Polym. Chem.* (2010) DOI:10.1039/b9py00244h
26. S. Ramesh, A.K. Arof, *Solid State Ionics* 136 - 137 (2000) 1197.
27. D. Golodnitsky, G. Ardel, E. Peled, *Solid State Ionics* 85 (1996) 231.
28. D.W. Kim, Y.R. Kim, J.K. Park, S.I. Moon, *Solid State Ionics* 106 (1998) 329.
29. S.H. Chung, P. Heitjans, R. Winter, W. Bzaucha, Z. Florjanczyk, Y. Onoda, *Solid State Ionics* 112 (1998) 153.